Anomalous length dependence of the conductance of graphene nanoribbons with zigzag edges

Ante Bili and Stefano Sanvito

Citation: The Journal of Chemical Physics **138**, 014704 (2013); doi: 10.1063/1.4773020
View online: http://dx.doi.org/10.1063/1.4773020
View Table of Contents: http://scitation.aip.org/content/aip/journal/jcp/138/1?ver=pdfcov
Published by the AIP Publishing

Anomalous length dependence of the conductance of graphene nanoribbons with zigzag edges

Ante Bilić[1,a)] and Stefano Sanvito[2]
[1]*CSIRO Mathematics, Informatics and Statistics, Private Bag 33, Clayton South 3169 VIC, Australia*
[2]*School of Physics and CRANN, Trinity College, Dublin 2, Ireland*

(Received 24 October 2012; accepted 7 December 2012; published online 3 January 2013)

Charge transport through two sets of symmetric graphene nanoribbons with zigzag shaped edges in a two-terminal device has been investigated, using density functional theory combined with the non-equilibrium Green's function method. The conductance has been explored as a function of nanoribbon length, bias voltage, and the strength of terminal coupling. The set of narrower nanoribbons, in the form of thiolated linear acenes, shows an anomalous length dependence of the conductance, which at first exhibits a drop and a minimum, followed by an evident rise. The length trend is shown to arise because of a gradual transformation in the transport mechanism, which changes from being governed by a continuum of out-of-plane π type and in-plane state channels to being fully controlled by a single, increasingly more resonant, occupied π state channel. For the set of nanoribbons with a wider profile, a steady increase is observed across the whole length range, owing to the absence of the former transport mechanism. The predicted trends are confirmed by the inclusion of self-interaction correction in the calculations. For both sets of nanoribbons the replacement of the strongly coupling thiol groups by weakly bonding phenathroline has been found to cause a strong attenuation with the length and a generally low conductance. © *2013 American Institute of Physics*. [http://dx.doi.org/10.1063/1.4773020]

I. INTRODUCTION

Graphene and closely related polycyclic aromatic hydrocarbons are materials of great interest to the scientific community.[1,2] While currently no alternative to the conventional metal-oxide-semiconductor based microelectronics has been identified, the potential to engineer the fundamental band gap and to control the charge flow has been demonstrated in the graphene meshes (for recent reviews see Refs. 3 and 4 and references therein). Recently, in an effort to identify suitable interconnects in nanodevices and molecular circuitry, charge transport through narrow graphene nanoribbons (GNRs) with armchair shaped edges, labeled 5-aGRNs,[4] has been investigated.[5] The findings of a consistently high conductance, nearly independent of the anchoring structure, the gold lead crystalline orientation, the nanoribbon length, and the bias voltage, make these GNRs almost ideal wires for molecular circuitry. The thiol terminal groups, commonly utilized for anchoring organic molecules to gold surfaces, provide a very strong bond with the leads. A subsequent study[6] of the conductance of amine-terminated 5-aGNRs, with weaker and more flexible bonds with gold, reported an even more unusual trend, which shows an increasing conductance with the length. GNRs with zigzag shaped edges have been much less investigated in this context, despite the predictions of metallic edges with magnetic ordering[7] and potential for spin polarized transport in future spintronics devices.[7,8] In fact, a serious doubt has recently been cast on the stability of the zGNRs outside ultrahigh vacuum pressures.[9]

Historically, the more common armchair edge of molecular wires has been dictated by the orientation of the prototypical molecular wire, benzene-1,4-dithiol (BDT), with the *para* substituted ring, in a gold breakpoint junction.[10] Another commercially available isomer, benzene-1,2-dithiol, with an *ortho* substitution, has been overlooked in this context, since, having two thiol groups adjacent to each other, it could not form a junction. However, assuming that both thiols chemisorb to a gold contact, this would make the benzene ring even more strongly adsorbed on the substrate on one side, while leaving the C-C bond on the opposite side open for further functionalization by thiols or other chemical groups and attachment to the opposite contact. The resulting hypothetical conformation thus exhibits multiple head groups, a condition that seems necessary for a high and stable conductance of GNRs,[5,6,11,12] and zigzag shaped edges, making it a representative of the 2-zGNRs[4] in a junction. The natural extension of benzene obtained by adding extra rings along the transport axis generates a series of 2-zGNRs known as linear acenes.

The thiol anchoring groups, frequently employed for the adsorption of organic molecules to gold surfaces, form a very strong, non-selective[13] bond with the electrodes. This is not desirable if, for example, one wishes to control the distance between points on the contacts at which the molecule is expected to attach. To circumvent this problem, more adaptable anchoring groups in the form of azines, that make weaker bonds with gold surfaces, have been proposed.[14–16] Junctions formed with amine-terminated molecules have demonstrated well defined, reproducible conductance histograms, with a narrow spread.[17] This is a consequence of the highly selective, yet flexible, amine-gold bonding nature. Very recently, a high

a)Author to whom correspondence should be addressed. Electronic mail: ante.bilic@csiro.au.

conductance has been predicted for 5-aGNRs with dual amine terminal groups.[6] The sp^3 hybridized N atoms in amines can still provide a substantial and directional bond with flat gold surfaces.[14,18] In contrast, a less directional and weaker bond is expected for the sp^2 hybridized N found in pyridine or in 1,10-phenanthroline.[15] In fact, the latter has been reported to make chemical bond with gold only via isolated Au adatoms that chelate the molecule to the surface.[16] Phenanthroline is potentially very interesting as a terminal group because its two anchoring N atoms are incorporated into the C backbone and they open up multiple transport pathways. Moreover, in the chemisorbed conformation the uppermost C-C bond is parallel to the surface and, hence, a further aromatization in the form of added benzene rings naturally produces adsorbates with zigzag shaped edges.

Here we report computational results on the conductance through two sets of nanoribbons, 2-zGNR and 4-zGNR, with both phenanthroline and dual thiol anchoring groups, as a function of the wire length and voltage bias. The shortest and longest considered geometries are shown in Fig. 1, optimized in a junction using Au(001) electrodes. The low molecular weight nanoribbons, known as linear acenes, pyrene, coronene, etc., are stable chemical compounds. Hence, the stability of monohydrogenated zigzag edges of these is preserved, perhaps unlike that of general zGNRs.[9] The 2-zGNR set with thiol anchors demonstrates an anomalous length trend of the conductance, manifested in drop and a minimum, followed by a rise. This is shown to arise because of a gradual transformation in the transport mechanism, which changes from that which is governed by a continuum of out-of-plane π type and in-plane state channels to that which is dominated by a single, increasingly more resonant, occupied π state channel. In contrast, the 4-zGNR set exhibits only the latter transport mechanism and, hence, a steady increase is predicted across the investigated length range. The substitution of the thiol anchor groups by weakly bonding phenathroline has been predicted to cause a strong attenuation with the length and a generally low conductance.

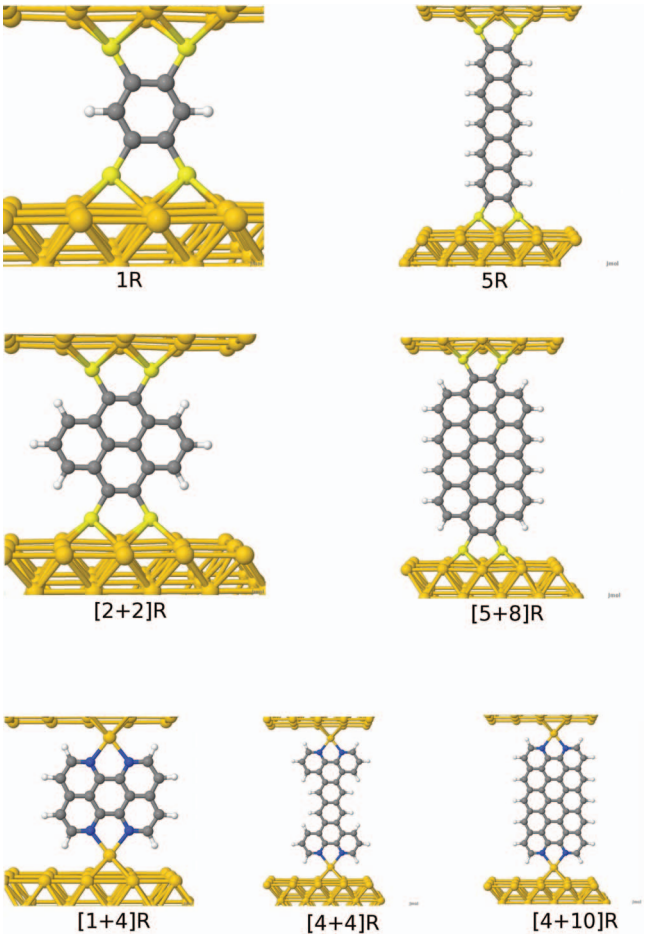

FIG. 1. The optimized junction geometries for the shortest and longest representatives from the considered series of GNRs. (Top row) 1R and 5R from the 2-zGNRs (i.e., linear acenes) with dithiol terminal groups. (Middle row) [2 + 2]R and [5 + 8]R from the 4-zGNRs with dithiol terminal groups. (Bottom row) [1 + 4]R, the common member of 2-zGNRs and 4-zGNRs, [4 + 4]R from the 2-zGNRs, and [4 + 10] from the 4-zGNRs with 1,10-phenathroline terminal groups.

II. METHODS

The present work adopts the computational approach that was previously utilized in the study of transport through the aromatic nanoribbons with armchair edges[5,6] and to a much lesser extent with zigzag edges.[12] The difference is that here spin-polarized calculations have been employed, due to the magnetic order previously predicted[7–9] for nanoribbons with zigzag edges. However, since the gold electrodes are not spin polarized, all the results are spin integrated. The geometries of all the junctions considered here have been fully optimized by conjugate gradients until the forces were smaller than 10 meV $Å^{-1}$. The optimizations were performed using density functional theory (DFT) as implemented in the SIESTA program.[19] The LDA functional[20] was used in both the DFT and transport calculations. The range of the atomic orbitals was evaluated based on an energy increase of 1 mRy arising due to the spherical confinement.

The optimized geometries obtained from the SIESTA computations, as well as all the relevant computational parameters, were subsequently employed in the electron transport calculations. The latter were conducted using the non-equilibrium Green's function (NEGF) Landauer approach[21] as implemented in the SMEAGOL package,[22–24] which is interfaced to SIESTA. Self interaction correction (SIC) can be applied to the scattering region of the junction to partly rectify the artifacts arising from the band misalignment between the wire and terminals.[25–28] Neither the local LDA or semilocal exchange-correlation functionals can predict *a priori* the band alignment between the leads and wire with the necessary accuracy. Hence, there would be no reason to prefer either class of functional in this regard. However, the important difference is that an implementation of SIC can be applied in combination with the LDA. In the present work this has been done by utilizing the atomic self interaction correction (ASIC).[29,30] A value of 1.0 was used for the scaling parameter α, amounting to the full ASIC.

Given the C_{2v} symmetry of the investigated nanoribbons, the Au(001) orientation of the leads, with a compatible symmetry, has been utilized. In this way the number of possible adsorption geometries for molecules with multiple anchoring

groups can be reduced to several highly symmetric representatives. The Au(001) surface was described by an extended rectangular superstructure of 15 gold atoms per layer, required by the large profile of 4-zGNRs. The Brillouin zone integrations were performed on a 2×1 k-point Monkhorst-Pack mesh in the plane of the contact surface. The (001) gold slab, 11 atomic layers thick, was partitioned by the boundaries of the supercell into two terminals, with 5 and 6 gold atomic layers on each side. The outer one or two layers of both contacts were taken as parts of the extended molecule, with which they form the scattering region (this is the part treated at the NEGF self-consistent level).

The thiol head groups readily form a strong bond with low index gold surfaces.[5,13] In contrast, 1,10-phenantroline forms a bond of substantial strength with gold via isolated gold adatoms.[16] The wires with phenathroline head groups have been connected to the terminals by attaching the head groups to the single adatoms on the opposite ends of the junction.

III. RESULTS AND DISCUSSION

A. Conductance of benzene-1,2,4,5-tetrathiol between Au(001) contacts

While at low coverages benzene-thiol preferentially adsorbs on the low index gold surfaces in almost flat orientations,[5,13] these conformations are not conducive to forming a junction with the two leads. Hence, the next most favorable adsorption conformation, i.e., upright with the S atoms placed at the hollow sites, is commonly considered as the prototypical molecular junction for 1,4-BDT. Accordingly, the adsorption of benzene-1,2,4,5-tetrathiol (1R) has been considered only with the molecular plane oriented perpendicular to the (001) gold surface. This mode of attachment results preferentially in a conformation with two adjacent S atoms bound to two adjacent hollow sites, two zigzag edges formed by the carbon backbone, and a large binding strength of 2.57 eV. The symmetric junction is established by anchoring the remaining two S atoms to the gold contact on the opposite side.

The *I-V* characteristics and zero-bias transmission coefficients for the 1R junction are shown in Fig. 2. The key feature is a very high, nearly bias-independent, conductance, which exceeds that of 1,4-BDT between Au(001) electrodes by a factor ranging between 2 and 4, depending on the anchoring site structure of the latter.[5] The corresponding transmission coefficient displays two prominent peaks, seen below and above the Fermi level, separated by a gap of approximately 3.5 eV. The peaks, however, although characteristic for aromatic wires (see, e.g., Fig. 5 in Ref. 31), in this case do not arise from the frontier molecular orbital, highest occupied (HOMO) and lowest unoccupied (LUMO), levels. In fact, the gap between them exhibits a rather flat continuum of conducting channels, a feature familiar to the related studies of transport by GNRs with dual thiol terminal groups.[5,12] Thus, despite the rather large gap between the peaks, the zero-bias conductance, defined by the transmission probability at the Fermi level, is quite high, 0.363 G_0 (e^2/h). To gain an insight

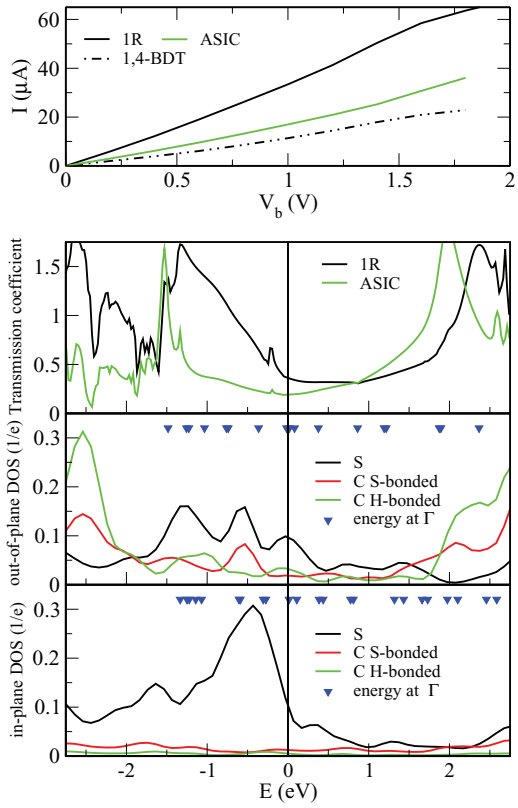

FIG. 2. (Upper panel) Current vs. bias voltage for the 1R wire between the Au(001) terminals. Results for the 1,4-BDT wire are also shown for reference. (Lower panels, from top to bottom) The zero-voltage transmission probability, the out-of-plane, and in-plane *p* orbital contribution to the partial density of states (PDOS) of the 1R wire. Only the LDA (ASIC-uncorrected) PDOS is shown. The blue triangles indicate the Γ point energies of the electronic states with the out-of-plane and in-plane symmetry. The energy is given relative to the Fermi level.

into the contributions that give rise to the transmission channels the projected density of states (PDOS) has been evaluated, also shown in Fig. 2. Only the components of the PDOS originating from the *p*-type atomic orbitals, out of the molecular plane and in-plane, for the three types of atoms forming the wire, S, S-bonded C, and H-bonded C. A relatively high degree of correlation between the transmission probability and the out-of-plane atomic contributions to PDOS underlines the importance of the out-of-plane π electronic states for charge transport. Visualization of the MOs at the Γ point reveals over a dozen out-of-plane π-type electronic states (not shown) in the -1.5 to 2.5 eV interval around the Fermi level, which captures both peaks and the continuum. Their energies are indicated by blue triangles in the PDOS panel. An analogous analysis of the in-plane PDOS components suggests that these electronic states, as expected, make a lesser contribution to the transmission. Individually they are much less effective due to the relatively small orbital density on the carbon backbone, in particular on the two central H-bonded C atoms. However, owing to the relatively large number of these states, about two dozen in the considered energy interval, they still make a significant contribution to the continuum of transmission channels. In summary, the high conductance of 1R is mainly a product of the very effective π conjugated system of out-of-plane states, which is amplified by the a host of less

efficient in-plane states. In addition, the dual head groups and short tunneling distance provide a very strong coupling across the entire junction.

B. Conductance of 2-zGNRs between Au(001) contacts

The *I*-*V* characteristics and the zero-bias transmission coefficients for the series of linear acenes, from naphthalene (2R) to pentacene (5R), or, equivalently, 2-zGNRs, are shown in Fig. 3. Several important observations can be made. Firstly, an evident drop in the conductance of 2R (relative to 1R, cf. Fig. 2) is extended by anthracene (3R) junction. However, for the next member, tetracene (4R), the current exhibits a slight increase. For 5R the rise is even more pronounced. Secondly, the transmission probability of 2R still largely resembles that of 1R in Fig. 2. The differences are manifested through a more subdued continuum of channels around the Fermi level for 2R and an emergence of a new distinct peak at 1.75 eV, which has split from the broad feature at 2.5 eV. Thirdly, for 3R the continuum has almost disappeared, thus accounting for the predicted conductance minimum. The peak on the occupied side of the 3R spectrum begins to develop a shoulder at −1 eV. In addition, the unoccupied state peak has shifted closer to the Fermi level. Finally, for 4R and even more so 5R, with the increasingly more conjugated C backbone, the spectra develop the familiar features in the form of two well defined peaks, one on each side of the charge neutrality level. For 5R the gap has been reduced to only 1.1 eV. Hence, the nature of charge transport has gradually changed from 1R, with a flat continuum of channels and an almost linear $I-V$ characteristic, to 5R, with an occupied state peak governing the zero-bias transport and an unoccupied state peak additionally contributing to the conductance for a voltage bias in excess of 0.7 eV.

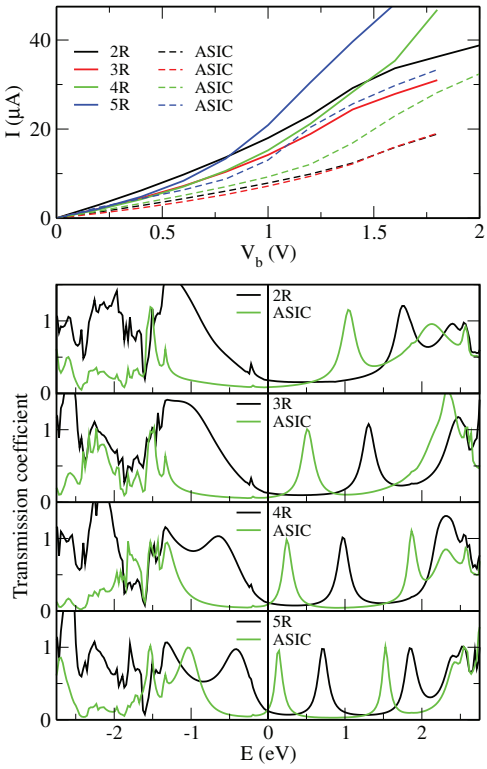

FIG. 3. (Upper panel) Current vs. bias voltage for the 2-3-4-5R series of 2-zGNRs with dithiol terminal groups between the Au(001) terminals. (Lower panels, from top to bottom) The zero-voltage transmission probability for the 2-3-4-5R junctions. The energy is given relative to the Fermi level.

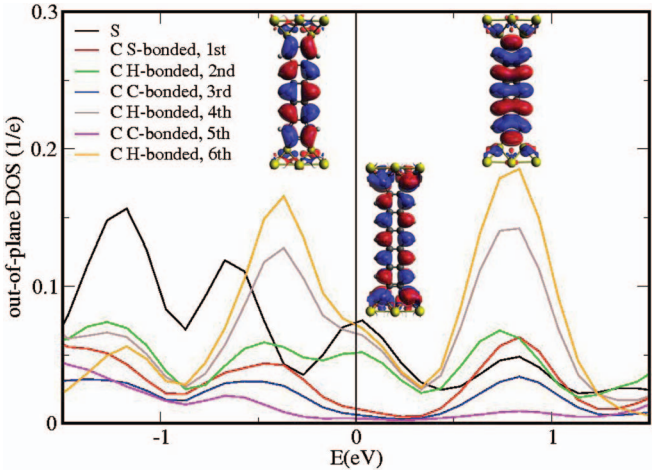

FIG. 4. The out-of-plane *p* orbital contribution to the partial density of states (PDOS) in the 5R junction from the S atom and six C atoms, whose respective row positions are labeled (from the 1st to the 6th). Only the LDA (ASIC-uncorrected) results are shown. The energy is given relative to the Fermi level. The orbital density at the Γ-point of the three π type states with peaks in the Fermi level vicinity are also shown.

The two peaks, at −0.4 and 0.7 eV, in the 5R transmission spectrum can be interpreted in terms of the out-of-plane PDOS atomic contributions at these energies, shown in Fig. 4. The first peak exhibits largest contributions from the outer, H-bonded, C atoms along the edge, in particular those that are closest to the middle of the junction (the sixth row of C atoms). The components from the inner, C-bonded, C atoms exhibit smaller amplitudes and follow the opposite ordering: those at the ends of the wire (the first and the last row of C atoms) contribute most. The corresponding electronic state at the Γ point is shown above the peak. It is worth noting that, owing to the antisymmetric nature with respect to the mirror plane σ_v perpendicular to the molecular plane, this state can be effectively harnessed by the dual terminal groups, away from the axis.[5,6] The S atoms display only moderate orbital contributions, but sufficient for a substantial coupling. The peak at 0.7 eV shows qualitatively the same atomic orbital contribution. However, the corresponding state at the Γ point shown above the peak displays left-right symmetry. It is interesting to note that the PDOS components from the S and outer, H-bonded C atoms exhibit another, smaller peak right at the Fermi level, which does not manifest in the transmission spectrum. The reason is that the inner, C-bonded C atoms do not substantially contribute to the DOS, which results in a poor overall conjugation. The corresponding electronic state at the Γ point, also shown above the peak, indeed displays nodes on the inner C atoms. Therefore, the low bias transport of 5R is controlled by the single occupied π state channel.

The DOS analysis accounts for the key contribution to the conductance of 5R, but it does not explain the lack of continuum channels evident in the 1R and 2R spectra. In order to understand the difference, the eleven in-plane electronic

states of the 5R junction at the Γ point in the relevant, −1 to 1 eV, energy interval have been visualized, shown in the top row of Fig. S1.[32] Clearly, the conjugation is completely broken across the three inner rings. This is why the continuum is still present in the spectrum of the 2R junction, but not for 3R. The in-plane Γ point orbitals for the 1R junction in the −1.5 to 2.5 eV energy range, labeled in the bottom panel of Fig. 2, are shown in the bottom three rows of Fig. S1. Most of them display a good conjugation across the entire junction, even though for some of them the conjugation is broken in the middle, on the H-bonded C atoms. Interestingly, the number (between 10 and 12) of the in-plane states in the −1 to 1 eV range does not seem to vary over the 1R–5R series of acenes. In contrast, the number of out-of-plane π states grows with the length, thus accounting for the smaller energy gap between the occupied and unoccupied states.

C. Conductance of 4-zGNRs between Au(001) contacts

Transport in the linear acenes is quasi one-dimensional, owing to the two pathways along the two edges, between which there is little, if any, charge exchange. This is due to their mirror symmetry and the transversal C-C bonds that connect them. In order to form proper graphene nanoribbons with a two-dimensional hexagonal scaffolding, one can laterally extend those wires by adding side rings. The smallest representation of a symmetric 4-zGNR is that of pyrene-3,4,8,9-tetrathiol, shown in Fig. 1, labeled [2 + 2]R henceforth, owing to the two central and two side rings. Recent findings demonstrate that the conductance of pyrene can vary by an order of magnitude, depending on the orientation in the junction, and that, by the extensions of the best performing pyrene motif, highly conductive GNRs can be formed.[12] The $I-V$ characteristics and the zero-bias transmission probability for the [2 + 2]R junction is shown in Fig. 5. Clearly, in this orientation pyrene displays about the lowest possible conductance (cf. Fig. 2 in Ref. 12), despite the dual terminal groups. This is a rather surprising result. Considering that the length of the wire is equal to that of 2R and given the two extra side rings, a lower band gap between occupied and unoccupied states is expected. This would normally result in superior transport properties. However, as shown in the second panel of Fig. 5, the [2 + 2]R transmission spectrum exhibits about the same gap as 2R, and, in addition, lacks the continuum of channels in the gap. Hence, despite the more graphene-like backbone, in the two terminal device [2 + 2]R performs much worse than 2R. In order to understand this apparent anomaly, out-of-plane and in-plane PDOS components have been evaluated and they are shown in Fig. 6. In general, the plots are very similar to those shown for 1R in Fig. 2. A closer look, however, reveals important differences. Firstly, the [2 + 2]R out-of-plane PDOS exhibits a visibly richer peak structure owing to the additional π type electronic states. However, some of these peaks in particular those around the Fermi level are conspicuously absent from the transmission spectrum in Fig. 5. The reason for this is the almost vanishing orbital contribution from the quartet of C atoms labeled 6, 8, 12, and 14 in Fig. 6 in the 0–1 eV energy range. Evidently, if these atoms,

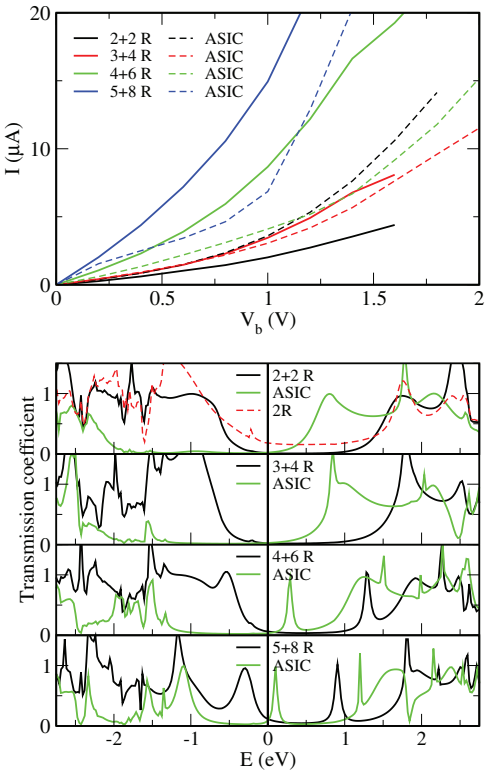

FIG. 5. (Upper panel) Current vs. bias voltage for the $[n + 2(n - 1)]$R, where $n = 2, 3, 4, 5$, series of 4-zGNRs with dithiol terminal groups between the Au(001) terminals. (Lower panels, from top to bottom) The zero-voltage transmission probability for these junctions. The energy is given relative to the Fermi level.

with a triple C coordination, do not contribute to a MO, both the available pathways, namely the one along the zigzag lines of the inner 2R and the one involving the perimeter of the C backbone, are disrupted at these sites. The latter pathway additionally suffers from the almost vanishing contribution from C atoms labeled 17 and 18 in the −0.5 to 1.8 eV energy range. This ineffective conjugation is the cause for the gap comparable to that of 2R. Secondly, the [2 + 2]R in-plane PDOS exhibits practically zero amplitudes on all but the S and S-bonded C atoms above the Fermi level. In fact, as the analysis of the in-plane electronic states at the Γ points indicates, only about half a dozen of these (not shown) across the whole energy range shown in the plot retain a reasonable, uninterrupted conjugation. Hence, the lack of continuum of conducting channels in the gap of the [2 + 2]R transmission spectrum is also a consequence of the poorly conjugated C backbone. The significance of this unexpected finding is that it demonstrates how a more extended graphene-like C backbone can have serious drawbacks for the overall conductivity.

The length dependence of the series of $[n + 2(n - 1)]$R wires, where $n = 2, \ldots, 5$, which comprises pyrene, coronene, and two longer members, is demonstrated in Fig. 5. As in the case of linear acenes of the same length (see Fig. 3), the emergence of well-defined isolated peaks on both sides of the Fermi level becomes evident with the extended length and conjugation of the out-of-plane π states, also manifested by the narrowing energy gap between them. The difference between the acenes and this series is the lack of continuum of

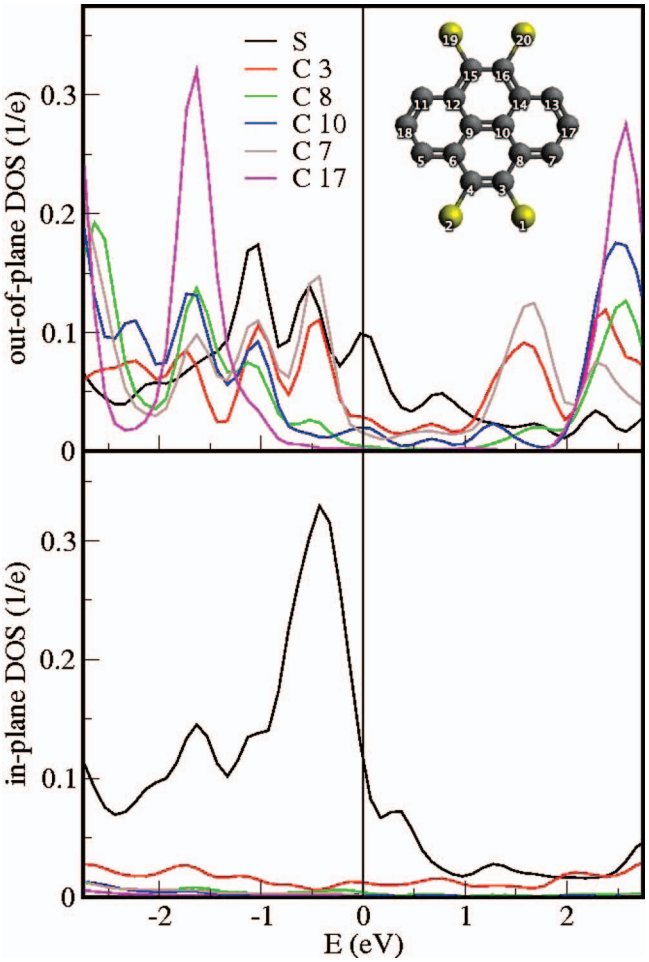

FIG. 6. The out-of-plane (top panel) and in-plane (bottom panel) p orbital contribution to the partial density of states (PDOS) for the $[2+2]$R wire. The labels of C atoms are indicated in the molecule backbone in the inset. Only the LDA results are shown. The energy is given relative to the Fermi level.

conducting channels for the short members of the latter set. Consequently, their conductance monotonically *rises* with the length. A similar result has recently been reported for the narrow armchair GNRs (5-aGNR type) with dual amine head groups.[6] However, it is worth noting that for the latter the ASIC-corrected low-bias current shows saturation. In contrast, the inclusion of ASIC in the present set simply moderates the current (in the case of $[2+2]$R it is actually amplified after the ASIC application), while the clear rising trend persists.

D. The effects of ASIC on the conductance of zGNRs

As evidenced from Figs. 2 and 3 for 2-zGNRs and Fig. 5 for 4-zGNRs the application of ASIC produces a significant down-shift of the energy levels of the frontier occupied states away from the charge neutrality level. The key effect of the larger energy disparity between the unchanged Fermi level and ASIC-corrected filled state levels is a dramatic reduction of their contribution to the transmission probability. Consequently the corrected gap in the zero-bias transmission spectrum appears visibly wider and, typically, a substantially lower conductance is predicted. This effect is partly offset by an even more evident, albeit smaller, down-shift of the frontier unoccupied states, closer to the charge neutrality level. In contrast to the effects of ASIC on occupied channels, the reduced energy difference between the Fermi level and corrected empty state levels amplifies their contribution to the transmission probability. As a consequence, it appears that the nature of conductance through the GNRs takes an increasingly more electronic form, as opposed to the uncorrected hole-like form, with the increasing nanoribbon length and conjugation. Note that the down-shift of the unoccupied energy levels is partly an artifact of the ASIC, since one does not expect a drift of empty states when the self interaction is removed from the filled electronic states. However, there is no way to properly optimize the energy levels of the unoccupied states in neither density functional or wavefunction theory, since there is no charge associated with them and, hence, they do not contribute to the total energy. The important quality of the ASIC is to retain the occupancy character of the electronic states so that, for example, the uncorrected energy of the lowest unoccupied state does not get below the Fermi level upon the application of ASIC. As we shall see in Subsection III E, that is not always the case. Finally, it is worth noting that the trends in the conductance with nanoribbon length indicated by the uncorrected calculations are preserved in the ASIC corrected results. Therefore, we conclude that the present predictions on the trends are generally robust against the artifacts of the exchange-correlation potential.

E. Conductance of 2- and 4-zGNRs with 1,10-phenantroline head groups

The $I-V$ characteristics and the zero-bias transmission probability for both the 2- and 4-zGNRs (i.e., the $[n+4]$R and $[n+2(n+1)]$R series, respectively, where $n=1,2,3,4$) with 1,10-phenantroline anchors are shown in Fig. 7. The common member, $[4+1]$R, is a heterocycle with a backbone in the shape of perylene, for which a very high conductance has been predicted with both thiol and amine head groups.[5,6] The important difference is the zigzag shaped edges in the current orientation, as opposed to the armchair edges in the previous reports, which, together with the anchoring N atoms being integrated in the backbone, substantially reduces the tunneling distance between the terminals. Hence, one could expect an even higher conductance in the present $[1+4]$R form. As Fig. 7 shows, a very high low-bias conductance is indeed predicted for $[1+4]$R, followed by much more moderated values at elevated biases. However, as the second panel indicates, the exceptional low-bias transport arises because of an isolated resonance nearly coinciding with the Fermi level. The analysis of out-of-plane PDOS components, shown in Fig. 8, indicates that this peak is a product of the electronic state that in the gas phase corresponds to the LUMO level, whose energy is predicted too low by the local and semi-local DFT functionals. The associated Γ point state in the junction is also shown in Fig. 8. The inherent problem of DFT band alignment between the metal contacts and extended conjugated molecule is particularly serious for weakly adsorbed wires with azine

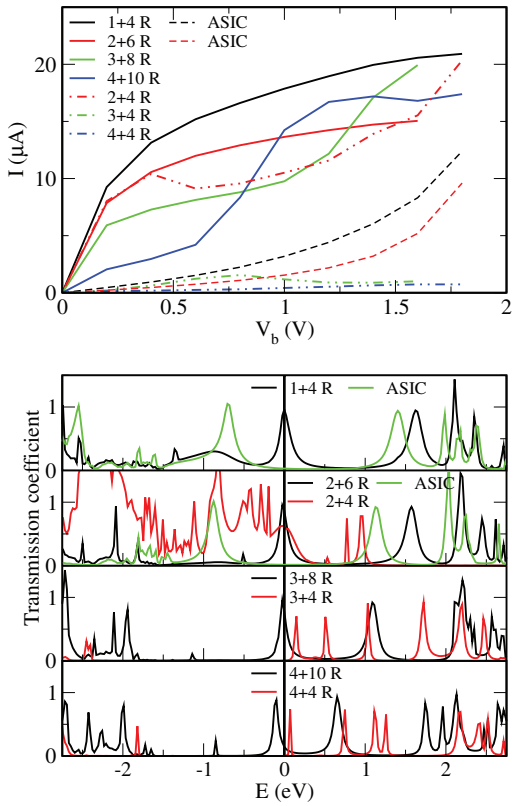

FIG. 7. (Upper panel) Current vs. bias voltage for the $[n + 4]$R and $[n + 2(n + 1)]$R, where $n = 1, 2, 3, 4$, series of 2- and 4-zGNRs, respectively, with phenanthroline terminal groups between the Au(001) terminals. (Lower panels, from top to bottom) The zero-voltage transmission probability for these junctions. The energy is given relative to the Fermi level.

anchors.[15,33] In order to rectify the large error in the HOMO-LUMO energy gap in benzene-1,4-diamine, empirical correction has been applied by Quek *et al.*[34] Recently, we have successfully employed the ASIC to partly correct the band alignment between gold and amine terminated 5-aGNRs.[6] However, in the case of 1,10-phenanthroline anchors, with weaker N-Au bonds due to the sp^2 hybridization of N, the inclusion of ASIC displays an undesirable effect. Namely, as the second panel in Fig. 7 shows, the energy of the LUMO resonance has been down-shifted to -0.7 eV, where it features as a fully occupied channel. The reason for this is probably the partially filled state of the resonance. In any case, the ASIC corrected low-bias conductance is an order of magnitude lower than the uncorrected value, which makes the $[1 + 4]$R a very poor wire. The conductance trend of the 4-zGNRs series, indicated by the uncorrected $I-V$ curves in Fig. 7, suggests that a rapid attenuation with length can be expected, which is the signature of non-resonant tunneling mechanism. The reason, as the lower panels demonstrate, is the shift of the Fermi level resonance deeper into the occupied range, even before the inclusion of ASIC. The application of ASIC to the transport via $[2 + 6]$R, resulting in a ca. 50% lower low-bias conductance, simply confirms the trend. Finally, for the 2-zGNRs wires (i.e., acenes) of the same length, even worse conductance is predicted, as shown in Fig. 7. Interestingly, for $[2 + 4]$R almost the same low-bias conductance has been evaluated as for the laterally extended $[2 + 6]$R. Even though $[2 + 4]$R is

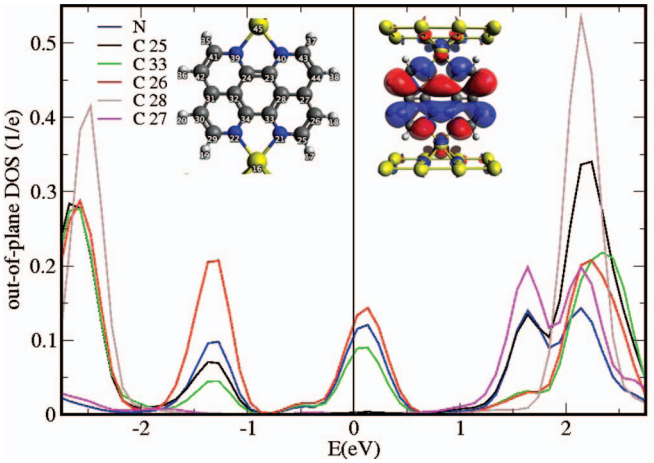

FIG. 8. The out-of-plane p orbital contribution to the partial density of states (PDOS) in the $[1 + 4]$R junction from the N atom and five C atoms. The labels of the C atoms are indicated in the molecule backbone in the inset. Only the LDA results are shown. The energy is given relative to the Fermi level. The orbital density at the Γ-point of the π type state with the peak at the Fermi level is also shown.

highly non-planar, due to a torsional twist caused by the steric repulsion between H atoms, the π type LUMO resonance exhibits a familiar resilience against the structural distortion.[31] In summary, both the zGNR series with phenanthroline terminal groups exhibit very poor conductance and rapid attenuation with length. Despite the highly conjugated C backbone of the zGNRs and inherent multiple transport pathways at the interface with metal contacts, provided by the dual pyridine rings, the weak coupling of the sp^2 hybridized N atoms with gold makes 1,10-phenanthroline unsuitable for use in molecular circuitry.

IV. CONCLUSIONS

In summary, we have investigated the conductance of two sets of symmetric aromatic nanoribbons, 2-zGNRs and 4-zGNRs, in a gold junction. The effects of nanoribbon length and the strength of terminal group bond to gold contacts have been investigated, with terminal groups that include weakly bonding phenanthroline and strongly coupling thiols. For the former anchors the increase in the wire length has been found to cause a strong attenuation in the conductance of both the series of nanoribbons. A combination of a low conductance and the unfavorable length effects makes phenanthroline a poorly suited linker group. In contrast, for the short thiol terminated 2-zGNRs an unusual length dependence is observed, with conductance at first exhibiting a drop as the mechanism of transport, dominated by a continuum of out-of-plane π type and in-plane state channels, rapidly weakens with the length. This is followed by another mechanism, which is controlled by a single filled π state channel and a rise in conductance with the length. Finally, for thiol terminated 4-zGNRs, owing to the complete absence of the continuum mediated transmission, an anomalous conductance, which monotonically increases with nanoribbon length, is predicted across the whole range. The inclusion of self-interaction correction in calculations confirms the trend. The results show that multiple transport pathway, inherent to phenanthroline backbone, do not

necessarily yield a superior conductivity. A strong coupling to the electrodes, provided by dual thiol groups, is essential to overcome the bottlenecks of the contact resistance, to provide the mechanical and thermal stability, and to fully harness the highly conjugated π type channels across the entire junction.

ACKNOWLEDGMENTS

This work was supported by the Flexible Electronics Theme of the CSIRO Future Manufacturing Flagship. A.B. thanks the CSIRO for support through the Julius Career Award. The use of the NCI National Facility supercomputers at the ANU is gratefully acknowledged. The SMEAGOL project is sponsored by Science Foundation of Ireland (Grant No. 07/IN/I945), by KAUST (FIC/2010/08) and by CRANN.

[1]A. K. Geim and K. S. Novoselov, Nature Mater. **6**, 183 (2007).
[2]J. Wu, W. Pisula, and K. Müllen, Chem. Rev. **107**, 718 (2007).
[3]A. H. Castro Neto, F. Guinea, N. M. R. Peres, K. S. Novoselov, and A. K. Geim, Rev. Mod. Phys. **81**, 109 (2009).
[4]S. M.-M. Dubois, Z. Zanolli, X. Declerc, and J.-C. Charlier, Eur. Phys. J. B **72**, 1 (2009).
[5]A. Bilić, J. D. Gale, and S. Sanvito, Phys. Rev. B **84**, 205436 (2011); **86**, 039905(E) (2012).
[6]A. Bilić and S. Sanvito, Phys. Rev. B **86**, 125409 (2012).
[7]Y.-W. Soon, M. L. Cohen, and S. G. Louie, Phys. Rev. Lett. **97**, 216803 (2006).
[8]Y.-W. Soon, M. L. Cohen, and S. G. Louie, Nature (London) **444**, 347 (2006).
[9]T. Wassmann, A. P. Seitsonen, A. M. Saita, M. Lazezeri, and F. Mauri, Phys. Rev. Lett. **101**, 096402 (2008).
[10]N. J. Tao, Nat. Nanotechnol. **1**, 173 (2006).
[11]A. Martin-Lasanta, D. Miguel, T. Garcia, J. A. Lopez-Villanueva, S. Rodriguez-Bolivar, F. M. Gomez-Campos, E. Bunuel, D. J. Cardenas, L. A. de Cienfugos, and J. M. Cuerva, Chem. Phys. Chem. **13**, 860 (2012).
[12]A. Bilić and S. Sanvito, "Tailoring highly conductive graphene nanoribbons from small polycyclic aromatic hydrocarbons: A pyrene study," J. Phys. Chem. C (submitted).
[13]A. Bilić, J. R. Reimers, and N. S. Hush, J. Chem. Phys. **122**, 094708 (2005).
[14]A. Bilić, J. R. Reimers, N. S. Hush, and J. Hafner, J. Chem. Phys. **116**, 8981 (2002).
[15]A. Bilić, J. R. Reimers, and N. S. Hush, J. Phys. Chem. B **106**, 6740 (2002).
[16]P. F. Cafe, A. G. Larsen, W. Yang, A. Bilic, I. M. Blake, M. J. Crossley, J. Zhang, H. Wackerbarth, J. Ulstrup, and J. R. Reimers, J. Phys. Chem. C **111**, 17285 (2007).
[17]L. Venkataraman, J. E. Klare, I. W. Tam, C. Nuckolls, M. S. Hybertsen, and M. L. Steigerwald, Nano Lett. **6**, 458 (2006).
[18]S. Piana and A. Bilic, J. Phys. Chem. B **110**, 23467 (2006).
[19]J. M. Soler, E. Artacho, J. D. Gale, A. García, J. Junquera, P. Ordejón, and D. Sánchez-Portal, J. Phys.: Condens. Matter **14**, 2745 (2002).
[20]D. M. Ceperley and B. J. Alder, Phys. Rev. Lett. **45**, 566 (1980).
[21]P. S. Damle, A. W. Ghosh, and S. Datta, in *Molecular Nanoelectronics*, edited by M. A. Reed and T. Lee (American Scientific, Los Angeles, 2003), p. 115.
[22]A. R. Rocha, V. M. Garcia-Suarez, S. W. Bailey, C. J. Lambert, J. Ferrer, and S. Sanvito, Nature Mater. **4**, 335 (2005).
[23]A. R. Rocha, V. M. Garcia-Suarez, S. W. Bailey, C. J. Lambert, J. Ferrer, and S. Sanvito, Phys. Rev. B **73**, 085414 (2006).
[24]I. Rungger and S. Sanvito, Phys. Rev. B **78**, 035407 (2008).
[25]C. Toher, A. Filippetti, S. Sanvito, and K. Burke, Phys. Rev. Lett. **95**, 146402 (2005).
[26]J. R. Reimers, G. C. Solomon, A. Gagliardi, A. Bilić, N. S. Hush, T. Frauenheim, A. D. Carlo, and A. Pecchia, J. Phys. Chem. A **111**, 5692 (2007).
[27]C. Toher and S. Sanvito, Phys. Rev. Lett. **99**, 056801 (2007).
[28]C. Toher and S. Sanvito, Phys. Rev. B **77**, 155402 (2008).
[29]C. D. Pemmaraju, T. Archer, D. Sánchez-Portal, and S. Sanvito, Phys. Rev. B **75**, 045101 (2007).
[30]A. Filippetti, C. D. Pemmaraju, S. Sanvito, P. Delugas, D. Puggioni, and V. Fiorentini, Phys. Rev. B **84**, 195127 (2011).
[31]A. Bilić, Ž. Crljen, B. Gumhalter, J. D. Gale, I. Rungger, and S. Sanvito, Phys. Rev. B **81**, 155101 (2010).
[32]See supplementary material at http://dx.doi.org/10.1063/1.4773020 for the plots of the orbital density of the in-plane electronic states in the −1 to 1 eV energy interval around the Fermi level at the Γ-point for the 5R junction. The in-plane electronic states in the −1.5 to 2.5 eV interval for the 1R junction, whose energies are labeled with blue triangles in the bottom panel of Fig. 2 are also shown therein.
[33]J. R. Reimers, Z. L. Cai, A. Bilić, and N. S. Hush, Ann. N.Y. Acad. Sci. **1006**, 235 (2003).
[34]S. Y. Quek, L. Venkataraman, H. J. Choi, S. G. Louie, M. S. Hybertsen, and J. B. Neaton, Nano Lett. **7**, 3477 (2007).